The Journal of Chemical Physics

# Local vibrational mode analysis of ion–solvent and solvent–solvent interactions for hydrated $Ca^{2+}$ clusters

Cite as: J. Chem. Phys. **153**, 224303 (2020); https://doi.org/10.1063/5.0034765
Submitted: 22 October 2020 . Accepted: 22 November 2020 . Published Online: 10 December 2020

Alexis A. A. Delgado, Daniel Sethio, Ipek Munar, Viktorya Aviyente, and Elfi Kraka

The Journal of Chemical Physics ARTICLE scitation.org/journal/jcp

# Local vibrational mode analysis of ion–solvent and solvent–solvent interactions for hydrated $Ca^{2+}$ clusters

Cite as: J. Chem. Phys. 153, 224303 (2020); doi: 10.1063/5.0034765
Submitted: 22 October 2020 • Accepted: 22 November 2020 •
Published Online: 10 December 2020



Alexis A. A. Delgado,[1] Daniel Sethio,[2] Ipek Munar,[3] Viktorya Aviyente,[3] and Elfi Kraka[1,a)]

## AFFILIATIONS

[1] Department of Chemistry, Computational and Theoretical Chemistry Group (CATCO), Southern Methodist University, 3215 Daniel Avenue, Dallas, Texas 75275-0314, USA
[2] Department of Chemistry - BMC, Uppsala University, Husargatan 3, 75237 Uppsala, Sweden
[3] Department of Chemistry, Boğaziçi University, Bebek 34342, Istanbul, Turkey

**Note:** This paper is part of the JCP Special Collection in Honor of Women in Chemical Physics and Physical Chemistry.
[a)] **Author to whom correspondence should be addressed:** ekraka@gmail.com

## ABSTRACT

Hydrated calcium ion clusters have received considerable attention due to their essential role in biological processes such as bone development, hormone regulation, blood coagulation, and neuronal signaling. To better understand the biological role of the cation, the interactions between the $Ca^{2+}$ ions and water molecules have been frequently investigated. However, a quantitative measure for the intrinsic Ca—O (ion–solvent) and intermolecular hydrogen bond (solvent–solvent) interactions has been missing so far. Here, we report a topological electron density analysis and a natural population analysis to analyze the nature of these interactions for a set of 14 hydrated calcium clusters via local mode stretching force constants obtained at the ωB97X-D/6-311++G(d,p) level of theory. The results revealed that the strength of inner Ca—O interactions for $\left[Ca(H_2O)_n\right]^{2+}$ (n = 1–8) clusters correlates with the electron density. The application of a second hydration shell to $\left[Ca(H_2O)_n\right]^{2+}$ (n = 6–8) clusters resulted in stronger Ca—O interactions where a larger electron charge transfer between lp(O) of the first hydration shell and the lower valence of Ca prevailed. The strength of the intermolecular hydrogen bonds, formed between the first and second hydration shells, became stronger when the charge transfers between hydrogen bond (HB) donors and HB acceptors were enhanced. From the local mode stretching force constants of implicitly and explicitly solvated $Ca^{2+}$, we found the six-coordinated cluster to possess the strongest stabilizations, and these results prove that the intrinsic bond strength measures for Ca—O and hydrogen bond interactions form new effective tools to predict the coordination number for the hydrated calcium ion clusters.



## I. INTRODUCTION

Calcium is the fifth most abundant element in the Earth's crust and is the most prominent alkaline earth metal in the human body.[1] In the Earth's crust, calcium is found in the form of carbonates, sulfates, and minerals such as calcite, aragonite, and gypsum.[2] In the human body, calcium is found in bone tissue and enamel in the form of calcium apatite or hydroxyapatite [i.e., HA, $Ca_{10}(OH)_2(PO_4)_6$].[3,4] Moreover, calcium is also found in intra- and extracellular fluids in the form of hydrated calcium clusters within the concentrations of 1 $\mu$M and 1 mM, respectively.[5] The weak ion–dipole interactions, which predominantly govern the interactions between the $Ca^{2+}$ ion and $H_2O$ molecules,[6,7] enable fast kinetics and high flexibility, which are both advantageous in controlling and maintaining many biological processes.[8] Hydrated calcium clusters are generally known for their essential involvement in bone development,[9–11] muscle contraction,[12,13] blood coagulation,[14] neuronal processes,[15–17] hormone and enzyme activation,[18] mitosis,[1] and cell death.[19] The capability of $Ca^{2+}$ ions to take on many forms of coordination gives rise to the diverse roles in structural, physiological, and biochemical processes.[20]

To illuminate the hydration process of the calcium ion, considerable attention has been directed toward the determination of the coordination number (CN). The CN is determined by the amount of water molecules, which directly bind to the $Ca^{2+}$ ion forming the electrostatic Ca—O interactions $\{[Ca(H_2O)_n]^{2+}$, where n is the number of $H_2O$ in the first hydration shell}. The results from experimental studies involving infrared multiple photon dissociation (IRMPD) spectroscopy,[21,22] collision induced dissociation (CID),[12] high pressure ion source mass spectrometer (HPMS),[23] and blackbody infrared radiative dissociation (BIRD)[24] have suggested a CN of 6 for the hydrated calcium clusters. The extended x-ray absorption fine structure spectroscopy (EXAFS) and large-angle x-ray scattering (LAXS) investigation using relatively high concentrations of four aqueous calcium halide solutions suggested a CN of 8 with the average Ca—O bond distances of 2.46 Å and 4.58 Å for the first and second hydration shells, respectively.[25] The EXAFS study conducted by Fulton *et al.* has suggested a CN of 7.2 ± 1.2 alongside a mean Ca—O bond distance of 2.44 Å.[26] Bruzzi and Stace via the application of the finite heat bath theory have reported experimental binding energies ranging from 14.8 kcal/mol to 29.9 kcal/mol for hydrated calcium clusters with a CN of 4–8.[27]

Theoretical studies involving Car–Parrinello molecular dynamics (CPMD) simulations,[28] density functional theory (DFT),[29,30] and second-order Møller–Plesset perturbation theory (MP2)[23] have suggested a CN of 6. Molecular dynamics (MD) simulations utilizing a hybrid quantum mechanics/molecular mechanics (QM/MM) method have suggested a CN in the range of 7.0–9.2.[31–33] CPMD simulations by Naor *et al.* concluded a CN in the range of 7–8.[34] Furthermore, a temperature dependent study involving DFT, MP2, and *ab initio* molecular dynamics simulations in dilute aqueous solutions has suggested a CN between 7 and 8 at low temperature and a CN of 6 at the ambient temperature.[35] However, a recent study utilizing Born–Oppenheimer molecular dynamics simulations has shown that the CN is not temperature dependent; a CN of 6 with an average Ca—O bond distance of 2.40 Å was observed over a wide range of temperature in their study.[36] Bai *et al.* and Lei *et al.* noted that the Ca—O bond distances increased along with the decrease in the charge of the $Ca^{2+}$ ion as the CN increased as revealed by the natural bond population orbital (NBO) analysis.[29,35] Merill *et al.* reported that the average bond orders of Ca—O decrease as the CN increases in parallel with the decrease in charge transfer from the $H_2O$ molecules to the $Ca^{2+}$ ion.[37] Although many experimental and computational studies have been performed, information about the intrinsic strength of ion–solvent (i.e., Ca—O) and solvent–solvent (i.e., hydrogen bonding between water molecules) interactions of hydrated calcium clusters is poorly understood. To the best of our knowledge, they have not been quantified due to the lack of a reliable intrinsic bond strength measure.

Binding energy (BE) is a valuable thermodynamic parameter for describing a chemical (i.e., hydration) process. It is also widely used as a bond strength measure, where the value is calculated by taking the energy differences between the cluster and its isolated components (i.e., the $Ca^{2+}$ ion and $H_2O$ molecules) in their equilibrium geometries. However, this value is heavily contaminated by electronic reorganizations and geometry relaxation of its fragments. Thus, it is of limited use as an ideal bond strength measure.[38–43] The local force constant ($k^a$) of a stretching vibration is the most suitable quantitative descriptor to probe the intrinsic strength without breaking any bonds/interactions; thus, the geometry and electronic structure are preserved.[44–47] The local stretching force constant is a reliable bond strength measure and has been successfully employed for describing covalent bonds[48–51] and noncovalent interactions including chalcogen bonding,[52] pnicogen bonding,[53] halogen bonding,[54–56] tetrel bonding,[57] and hydrogen bonding.[58–63]

The quantitative description of the ion–solvent and solvent–solvent interactions is important for understanding the hydration of $Ca^{2+}$ ions, and the detailed knowledge of the interactions that stabilize the hydrated calcium clusters is key to better understand the biological role of the cation. In this work, for the first time, we employed the local mode analysis developed by Konkoli and Cremer as an ideal bond strength measure to quantify the electrostatic interactions between the $Ca^{2+}$ ion and $H_2O$ molecules (Ca—O) and the hydrogen bonding between water molecules of the first and second hydration shells. The main objectives of this work are as follows: (i) to evaluate the intrinsic strength of ion–solvent (Ca—O) interactions and their modulation as the CN increases from 1 to 8 in the first hydration shell $\{[Ca(H_2O)_n]^{2+}$, where n = 1–8}, (ii) to determine the effect of an additional hydration shell on the intrinsic strength of inner Ca—O interactions $\{[Ca(H_2O)_n]^{2+} - m(H_2O)$ with n = 1–8, m = 1–4 and n + m = 9 or 10, where m is the amount of water molecules in the second hydration shell}, and (iii) to quantify intermolecular hydrogen bonding occurring between the first and second hydration shells.

## II. COMPUTATIONAL METHODS

Equilibrium geometries and normal vibrational modes of 14 hydrated calcium clusters and reference molecules **R1**–**R5** were obtained using the $\omega$B97X-D functional[64–66] in combination with Pople's 6-311++G(d,p) basis set of triple-$\zeta$ quality.[67,68] The dispersion corrected $\omega$B97X-D functional was chosen as it is known to accurately and consistently describe clusters that are governed by noncovalent interactions (NCIs)[69,70] including hydrogen bond interactions.[71–73] Clusters **1**–**8** and reference molecules **R1** and **R2** were recalculated at the same level of theory where the water solvation effects for the outer hydration shells were assessed using the explicit conductor-like polarizable continuum model (CPCM). The explicit CPCM model was chosen as it has shown reasonable success.[74,75] The initial structures of clusters **1**–**8** were taken from the work of Lei and Pan.[29] The initial structures of clusters **9**–**14** were taken from the work of Bai *et al.*[35]

After geometry and vibrational frequency calculations, the local mode analysis (LMA) of Konkoli and Cremer[44–47] based on vibrational spectroscopy was utilized to quantify the intrinsic strength of the ion–solvent interactions in the first hydration shell along with the solvent–solvent interactions occurring between the first and second hydration shells.

Vibrational spectroscopy provides invaluable information about the electron structure of a molecule and its intrinsic strength. However, the direct use of the information encoded within normal vibrational modes cannot be directly used to describe the strength of chemical bonds. This is due to the delocalized nature of normal vibrational modes resulting from electronic and kinematic (mass)

coupling. The electronic coupling caused by off-diagonal elements of the force constant matrix $\mathbf{F}^q$ is eliminated by solving the Wilson equation,[76]

$$\mathbf{F}^q\mathbf{D} = \mathbf{G}^{-1}\mathbf{D}\Lambda, \tag{1}$$

where $\mathbf{F}$ represents the force constant matrix, which is expressed by 3 K (K is the number of atoms) in internal coordinates $q$, $\mathbf{D}$ is the eigenvector matrix consisting of vibrational eigenvectors $\mathbf{d}_\mu(\mu = 1, \ldots N_{vib})$ given in column vectors, $\mathbf{G}$ is the Wilson mass-matrix, and $\Lambda$ is the diagonal matrix consisting of vibrational eigenvalues $\lambda_\mu$ ($\lambda_\mu = 4\pi^2c^2\omega_\mu^2$, $c$ = speed of light, and $\omega_\mu$ = harmonic vibrational frequencies in $cm^{-1}$ of the normal mode vectors $\mathbf{d}_\mu$). The solution of Eq. (1) yields the diagonal force constant matrix $\mathbf{K}$ expressed in normal coordinates $\mathbf{Q}$, which is free from electronic coupling,

$$\mathbf{K}^Q = \mathbf{D}^\dagger\mathbf{F}^q\mathbf{D}. \tag{2}$$

Konkoli and Cremer showed that the remaining kinematic (mass) coupling can be eliminated by solving mass-decouple Euler–Lagrange equations.[44–47] The resulting local vibrational modes ($\mathbf{a}_n$), which are free from any mode–mode coupling, can be obtained via

$$\mathbf{a}_n = \frac{\mathbf{K}^{-1}\mathbf{d}_n^\dagger}{\mathbf{d}_n\mathbf{K}^{-1}\mathbf{d}_n^\dagger}, \tag{3}$$

where $\mathbf{a}_n$ is the local mode vector associated with the $n$th internal coordinate $q_n$. Every local mode $\mathbf{a}_n$ corresponds to a unique local mode force constant $k_n^a$, which is derived by the following equation:

$$k_n^a = \mathbf{a_n^\dagger K a_n} = \left(\mathbf{d}_n\mathbf{K}^{-1}\mathbf{d}_n^\dagger\right)^{-1}. \tag{4}$$

Zou and Cremer showed via an adiabatic connection scheme (ACS) that there is a one-to-one relationship between local vibrational modes and normal vibrational modes.[47,77] From the local modes $k_n^a$, the local vibrational frequencies $\omega_n^a$ are obtained through

$$\left(\omega_n^a\right)^2 = \frac{1}{4\pi^2c^2}k_n^aG_{n,n}^a, \tag{5}$$

where the mass of the local mode $\mathbf{a}_n$ is represented by $G_{n,n}^a$, which is a diagonal element of the Wilson $\mathbf{G}$ matrix.

The resulting local mode force constants $k_n^a$ are independent of the type of coordinates used for the molecular description in contrast to their normal mode counterparts. Relying solely on the changes in the electronic structure, local mode force constants provide a reliable bond strength measure, which further can be transformed into bond strength orders using a generalized Badger rule,[78]

$$\text{BSO } n = a\left(k^a\right)^b. \tag{6}$$

Note that, hereafter, we use $k^a$ for representing $k_n^a$ (i.e., $k^a = k_n^a$). The constants a and b were obtained using two reference molecules, which have well-defined bond orders, and the assumption of $k^a = 0$ for BSO $n = 0$. For the Ca—O interactions, $CaH_2$ (**R1**) and Ca=O (**R2**) were used as reference molecules with corresponding BSO $n$ values of 1.0 and 2.0, respectively. The $a$ and $b$ constants derived using **R1** and **R2** are 1.0137 and 0.4799. For the Ca—O interactions using the CPCM model, the $a$ and $b$ constants derived from **R1** and **R2** are 1.4729 and 0.5057. For HBs, F—H (**R3**) and $[H\cdots F\cdots H]^-$ (**R4**) were used as reference molecules with BSO $n$ values of 1.0 and 0.5, respectively. The $a$ and $b$ constants derived using **R3** and **R4** are 0.5293 and 0.2781. For comparison, we also calculated the intrinsic strength of hydrogen bonding of the water dimer (**R5**).

Binding energies (BEs) were calculated by taking the energy differences between the hydrated calcium cluster and its isolated components in their equilibrium geometries,

$$\begin{gathered} Ca^{2+} + nH_2O \rightarrow \left[Ca(H_2O)_n\right]^{2+}, \\ BE = E_{\left[Ca(H_2O)_n\right]^{2+}} - E_{Ca^{2+}} - n.E_{H_2O}, \\ \left[Ca(H_2O)_n\right]^{2+} - m(H_2O) \rightarrow Ca^{2+} + n\text{–}mH_2O, \end{gathered} \tag{7}$$

where the binding energy of the clusters with a second hydration shell was calculated using

$$BE = E_{\left[Ca(H_2O)_n\right]^{2+}\text{–}m(H_2O)} - E_{(H_2O)_n\text{–}m(H_2O)} - E_{Ca^{2+}}. \tag{8}$$

All DFT calculations were performed using the Gaussian 16 Rev. C.01 package.[79] Geometry optimizations were carried out with a super-fine grid integration and a tight convergence criterion for the forces and displacements. The local vibrational force constants were obtained via the local mode analysis using the COLOGNE2019 program.[80] Natural population charges and second order perturbation stabilization energy [$\Delta E^{(2)}$] due to orbital interactions were obtained from the natural bond orbital (NBO) analysis using the NBO6 program.[81,82]

The electron density ($\rho_c$) and energy density ($H_c$) at Ca—O and O···H bond critical points $r_c$ were calculated using the AIMALL program.[83] Following the Cremer–Kraka criteria, the nature of the Ca—O and HB interactions was characterized through the energy density $H_c$ at the bond critical point $r_c$(BCP). Covalent bonding is indicated by a negative (stabilizing) value of the energy density ($H_c < 0$), while electrostatic interactions are indicated by $H_c > 0$.[84–86]

## III. RESULTS AND DISCUSSION

In the following, the results of 14 hydrated calcium clusters are presented. First, the strength of ion–solvent (Ca—O) interactions in the first hydration shell (clusters **1**–**8**) is discussed. Second, the strength of solvent–solvent (hydrogen bond) interactions occurring between the first and second hydration shells (clusters **9**–**14**) is discussed in parallel to the modulation of Ca—O bond strengths resulting from the addition of a second hydration shell. Third, the use of local vibrational mode analysis as a predictive tool for determining the coordination number of hydrated calcium clusters is presented.

### A. First hydration shell

Table I summarizes bond distances (R), local vibrational frequencies ($\omega^a$), local mode force constants ($k^a$), bond strength orders

**TABLE I**. Bond distances (R), local mode frequencies ($\omega^a$), local mode force constants ($k^a$), bond strength orders (BSOs $n$), electron densities ($\rho_c$), energy densities ($H_c$), and the energy density ratios ($\frac{H_c}{\rho_c}$) of Ca—O interactions for clusters **1–14** and reference molecules **R1** and **R2**, calculated at the ωB97X-D/6-311++G(d,p) level of theory.[a]

| No. | Molecule | Sym. | R (Å) | $\omega^a$ ($cm^{-1}$) | $k^a$ (mdyn/Å) | BSOs $n$ | $\rho_c$ ($e/Å^3$) | $H_c$ ($h/Å^3$) | $\frac{H_c}{\rho_c}$ ($h/e$) |
|---|---|---|---|---|---|---|---|---|---|
| | *First Hydration Shell* | | | | | | | | |
| 1 | $[Ca(H_2O)]^{2+}$ | $C_{2v}$ | 2.251 | 413 | 1.147 | 1.083 | 0.314 | 0.043 | 0.137 |
| 2 | $[Ca(H_2O)_2]^{2+}$ | $C_2$ | 2.287 | 388 | 1.012 | 1.020 | 0.285 | 0.043 | 0.152 |
| 3 | $[Ca(H_2O)_3]^{2+}$ | $D_3$ | 2.316 | 365 | 0.895 | 0.961 | 0.264 | 0.043 | 0.164 |
| 4 | $[Ca(H_2O)_4]^{2+}$ | $S_4$ | 2.339 | 360 | 0.873 | 0.950 | 0.247 | 0.044 | 0.176 |
| 5 | $[Ca(H_2O)_5]^{2+}$ | $C_{2v}$ | 2.366 | 331 | 0.741 | 0.878 | 0.231 | 0.043 | 0.186 |
| 6 | $[Ca(H_2O)_6]^{2+}$ | $O_h$ | 2.388 | 296 | 0.589 | 0.786 | 0.217 | 0.042 | 0.192 |
| 7 | $[Ca(H_2O)_7]^{2+}$ | $C_2$ | 2.440 | 253 | 0.432 | 0.678 | 0.192 | 0.040 | 0.207 |
| 8 | $[Ca(H_2O)_8]^{2+}$ | $D_4$ | 2.486 | 225 | 0.341 | 0.605 | 0.170 | 0.035 | 0.209 |
| | *Second Hydration Shell* | | | | | | | | |
| 9 | $[Ca(H_2O)_6]^{2+} - 3(H_2O)$ | $D_3$ | 2.376 | 316 | 0.671 | 0.837 | 0.224 | 0.043 | 0.190 |
| 10 | $[Ca(H_2O)_6]^{2+} - 4(H_2O)$ | $C_1$ | 2.377 | 290 | 0.573 | 0.770 | 0.224 | 0.042 | 0.190 |
| 11 | $[Ca(H_2O)_7]^{2+} - 2(H_2O)$ | $C_2$ | 2.427 | 263 | 0.468 | 0.704 | 0.196 | 0.040 | 0.205 |
| 12 | $[Ca(H_2O)_7]^{2+} - 3(H_2O)$ | $C_1$ | 2.426 | 263 | 0.468 | 0.704 | 0.197 | 0.040 | 0.204 |
| 13 | $[Ca(H_2O)_8]^{2+} - (H_2O)$ | $C_2$ | 2.480 | 218 | 0.323 | 0.587 | 0.172 | 0.036 | 0.209 |
| 14 | $[Ca(H_2O)_8]^{2+} - 2(H_2O)$ | $D_2$ | 2.476 | 224 | 0.339 | 0.601 | 0.174 | 0.036 | 0.208 |
| | **Ca—O bond references** | | | | | | | | |
| R1 | $CaH_2$ | $D_{\infty h}$ | 2.051 | 1296 | 0.972 | 1.000 | 0.320 | −0.044 | −0.137 |
| R2 | Ca—O | $C_{\infty v}$ | 1.825 | 782 | 4.120 | 2.000 | 0.967 | −0.220 | −0.277 |

[a]The values were taken as averages over all Ca—O interactions.

(BSOs $n$), electron densities ($\rho_c$), energy densities ($H_c$), and energy density ratios ($H_c/\rho_c$) for Ca—O interactions taken as averages over all Ca—O interactions of clusters **1–14**. Calculated molecular geometries, point group symmetries, and selected NBO charges are depicted in Fig. 1. To differentiate the water molecules in the first and second hydration shells, we use the $[Ca(H_2O)_n]^{2+} - m(H_2O)$ notation, where n and m refer to the number of water molecules in the first and second hydration shells, respectively. In regard to the plots, red points correspond to $[Ca(H_2O)_n]^{2+}$ clusters, and green points refer to $[Ca(H_2O)_n]^{2+} - m(H_2O)$ clusters. Although the CN of hydrated calcium clusters has been suggested to range between 5 and 9, for the sake of completeness, we investigate clusters where the CN ranges from 1 to 9. It is noteworthy that the optimization of the $[Ca(H_2O)_9]^{2+}$ cluster resulted in the migration of one water molecule from the first hydration shell to the second hydration shell, which is in agreement with previous findings.[30,35,87]

The Ca—O bond lengths for clusters **1–8** increase from 2.251 Å in cluster **1** to 2.486 Å in cluster **8**. This observation agrees with previous findings where Ca—O bond lengths of clusters **1–8** steadily increase from 2.24 to 2.57 Å as the amount of water molecules in the first hydration shell increase. It is worth noting that the Ca—O bond distances of clusters **6–8** are in agreement with the experimental Ca—O bond distances determined by EXAFS and LAXS.[26] In addition, according to the Cremer–Kraka criterion,[84–86] all Ca—O interactions are electrostatic in nature.

The average BSO $n$ values of the Ca—O interactions for clusters **1–8** are compared in Fig. 2. The average BSO $n$ values of Ca—O interactions range from 1.083 to 0.605; as the CN of hydrated calcium clusters increases, the BSO $n$ of the Ca—O interactions decreases. The Ca—O interactions of clusters **3–8** become weaker, where those of **6–8** are significantly weaker than the Ca—H bond of the reference molecule ($CaH_2$, **R1**). The second order perturbation of the Fock matrix analysis reveals that the charge transfer from the lone pair (lp) of the O atom of the $H_2O$ molecule to the lower valence (lv) of the Ca ion is responsible for the decrease in the NBO charge for Ca and O atoms. The NBO charges of the Ca and O atoms decrease steadily as the CN increases due to larger charge transfers between lp(O) and the Ca ion (see Table S4), which translates to weaker Ca—O electrostatic interactions. Moreover, as the CN increases, the electron density at the Ca—O bond critical point decreases, correlating with a decrease in the Ca—O bond strength (see Figs. 3).

## B. Second hydration shell

Table II summarizes bond distances (R), local vibrational frequencies ($\omega^a$), local mode force constants ($k^a$), bond strength orders (BSOs $n$), electron densities ($\rho_c$), energy densities ($H_c$), and their ratio ($H_c/\rho_c$) for hydrogen bonds taken as averages over all hydrogen bonds of clusters **9–14**. Clusters **9–14** possess both ion–solvent (Ca—O) and solvent–solvent (hydrogen bonding) interactions. The $H_2O$ molecules of the first water shell interact with those of the

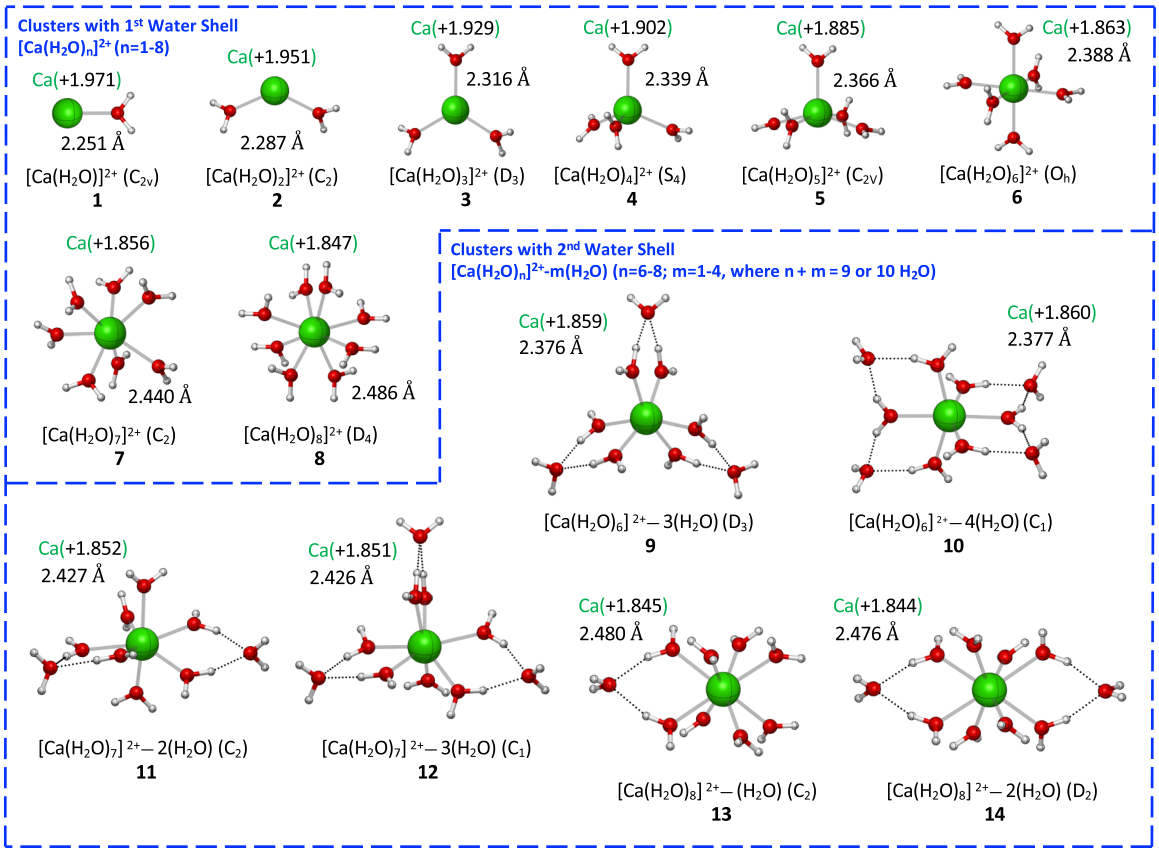


**FIG. 1**. Natural bond orbital (NBO) charges for the Ca atom and Ca—O bond distances for all clusters obtained at the $\omega$B97X-D/6-311++G(d,p) level of theory.

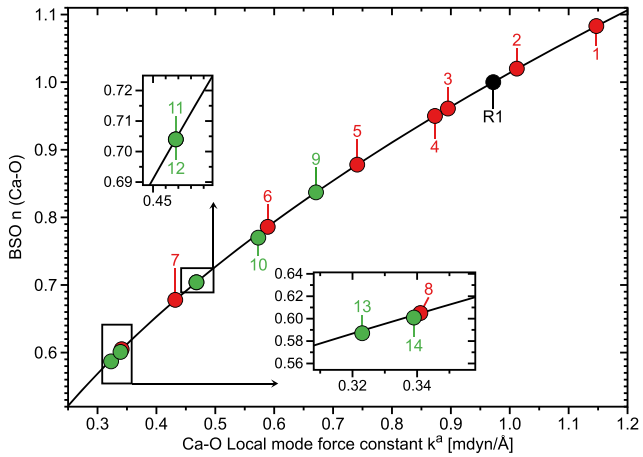


**FIG. 2**. BSO $n$ (Ca—O) values and Ca—O force constants $k^a$ for clusters **1**–**14** and **R1** calculated at the $\omega$B97X-D/6-311++G(d,p) level of theory. BSO $n$ (Ca—O) values were calculated via Eq. (6). **R2** was excluded from the plot to improve visibility of the data.

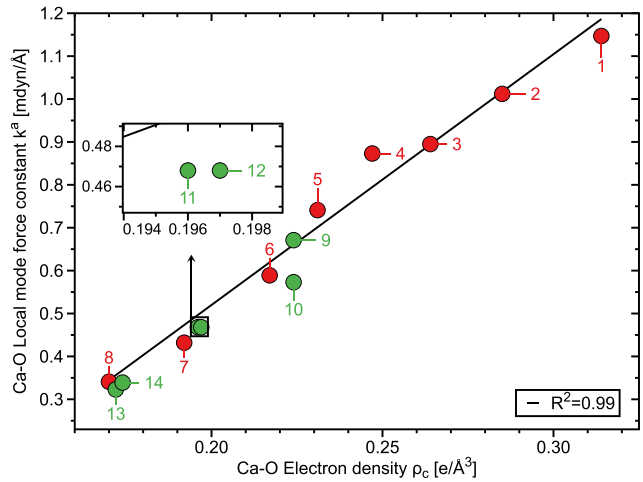


**FIG. 3**. The Ca—O force constants $k^a$ vs the Ca—O electron densities $\rho_c$ for clusters **1**–**14** calculated at the $\omega$B97X-D/6-311++G(d,p) level of theory.

**TABLE II**. Bond distances (R), local mode frequencies ($\omega^a$), local mode force constants ($k^a$), bond strength orders (BSOs $n$), electron densities ($\rho_c$), energy densities ($H_c$), and the energy density ratios ($\frac{H_c}{\rho_c}$) for hydrogen bonds (O···H) of clusters **9**–**14** and reference molecules **R3** and **R5**, calculated at the $\omega$B97X-D/6-311++G(d,p) level of theory.[a]

| No. | Molecule | Sym. | R (Å) | $\omega^a$ ($cm^{-1}$) | $k^a$ (mdyn/Å) | BSOs $n$ | $\rho_c$ ($e/Å^3$) | $H_c$ ($h/Å^3$) | $\frac{H_c}{\rho_c}$ ($h/e$) |
|---|---|---|---|---|---|---|---|---|---|
| 9 | $[Ca(H_2O)_6]^{2+} - 3(H_2O)$ | $D_3$ | 1.858 | 592 | 0.196 | 0.336 | 0.197 | 0.010 | 0.051 |
| 10 | $[Ca(H_2O)_6]^{2+} - 4(H_2O)$ | $C_1$ | 1.877 | 555 | 0.173 | 0.324 | 0.189 | 0.012 | 0.062 |
| 11 | $[Ca(H_2O)_7]^{2+} - 2(H_2O)$ | $C_2$ | 1.862 | 599 | 0.200 | 0.338 | 0.195 | 0.011 | 0.054 |
| 12 | $[Ca(H_2O)_7]^{2+} - 3(H_2O)$ | $C_1$ | 1.872 | 577 | 0.186 | 0.331 | 0.191 | 0.012 | 0.060 |
| 13 | $[Ca(H_2O)_8]^{2+} - (H_2O)$ | $C_2$ | 1.873 | 575 | 0.185 | 0.331 | 0.190 | 0.011 | 0.060 |
| 14 | $[Ca(H_2O)_8]^{2+} - 2(H_2O)$ | $D_2$ | 1.878 | 563 | 0.177 | 0.327 | 0.188 | 0.012 | 0.064 |
| | **HB references** | | | | | | | | |
| R3 | $[FH_2]^-$ | $D_{\infty v}$ | 1.142 | 1202 | 0.815 | 0.500 | 1.180 | −1.316 | −1.115 |
| R4 | FH | $C_{\infty v}$ | 0.917 | 4180 | 9.854 | 1.000 | 2.544 | −5.471 | −2.150 |
| | **HB of the water dimmer** | | | | | | | | |
| R5 | $(H_2O)_2$ | $C_s$ | 1.916 | 615 | 0.211 | 0.343 | 0.173 | 0.015 | 0.089 |

[a]The values were taken as averages over all hydrogen bonds.

second hydration shell through hydrogen bonds (HBs). As shown in Fig. 1, the HBs occur between an electropositive H atom of the $H_2O$ molecule in the first hydration shell and an electronegative O atom of the $H_2O$ molecule in the second hydration shell,[12] where the H atom in the first hydration shell acts as a HB donor and the O atom in the second hydration shell acts as a HB acceptor. For clusters **9**–**14**, the distance of inner and outer Ca—O interactions ranges from 2.376 Å to 2.480 Å and 4.200 Å to 5.029 Å, respectively, which are in good agreement with the previous experimental study by EXAFS and LAXS experiments [inner: 2.46(1) Å–2.46(2) Å and outer: 4.58(5) Å].[25] Moreover, our results are also in agreement with the computational work of Bai *et al.*, which suggests inner Ca—O bond distances for **9**–**14** to range between 2.381 and 2.493 Å.[35]

Cluster **9** possesses six and three water molecules in the first and second hydration shells $\{[Ca(H_2O)_6]^{2+} - 3(H_2O)\}$, respectively. The three water molecules of the second hydration shell are bonded to the water molecules of the first hydration shell via six O—H···O HB interactions with a BSO $n$ average of 0.336 ($k^a$ = 0.196 mdyn/Å). According to the Cremer–Kraka criterion,[84–86] all HBs in cluster **9** are electrostatic in nature. The HBs of cluster **9** are weaker, on average, than the HB of the water dimer (BSO $n$: 0.343, $k^a$: 0.211 mdyn/Å). The NBO analysis reveals that the charge transfer from second shell water molecules to the first shell water molecules increases the charge belonging to the O atoms of the inner hydration shell; this increase in the charge strengthens the Ca—O electrostatic interactions of **9**. The average (inner) Ca—O bond distance for cluster **9** is shorter by 0.012 Å and stronger by 0.082 mdyn/Å in contrast to that of cluster **6**. As well, the Ca—O interactions of **9** are the strongest among clusters, which posses two hydration shells (clusters **9**–**14**) (see Table I).

Cluster **10** contains six and four water molecules in the first and second hydration shells $\{[Ca(H_2O)_6]^{2+} - 4(H_2O)\}$, respectively. The four water molecules of the outer hydration shell are bonded to the inner hydration shell by forming eight HB interactions with average BSO $n$ values of 0.324 ($k^a$ = 0.173 mdyn/Å). The HB interactions of cluster **10** are longer and weaker compared to the HBs of cluster **9** (see Table II). Previous study by Tao *et al.* has shown that the interaction between lp(O) of the HB acceptor and $\sigma^*$(O—H) of the HB donor of the water dimer is the most stabilizing factor and that the strength of HB interactions for hydrogen bonded complexes is governed by push–pull effects, which can be elucidated via enhanced charge transfer.[88] In general, the more charge transfer a HB has, the stronger the HB interaction.[88] The average stabilization energy values [$\Delta E^{(2)}$], due to the charge transfer from the O atoms of the second hydration shell to the $\sigma^*$(O—H) orbitals of the first hydration shell, reveal that HBs of cluster **10** are weaker than those of cluster **9** due to smaller electron charge transfers [$\Delta E^{(2)}$ = 4.290 (**9**); 3.940 kcal/mol (**10**)]. Furthermore, the HB electron density values are greater for cluster **9** with respect to **10** [$\rho_c$ = 0.197 (**9**), 0.189 e/Å$^3$ (**10**)]. The Ca—O interactions of cluster **10** (R: 2.377 Å, BSO $n$: 0.770) are longer and weaker than those of cluster **9** (R: 2.376 Å, BSO $n$: 0.837) as a result of weaker electrostatic interactions between the Ca ion and O atoms of the first hydration shell, which is attributed to a smaller amount of electron charge transfer from lp(O) of $H_2O$ to the lower valence (lv) of the Ca ion [$\Delta E^{(2)}$ = 14.94 (**9**); 13.57 kcal/mol (**10**)].

Cluster **11** consists of seven water molecules in the first hydration shell and two water molecules in the second hydration shell $\{[Ca(H_2O)_7]^{2+} - 2(H_2O)\}$. Two water molecules of the second shell form four HB interactions with water of the first shell with an average BSO $n$ of 0.338 ($k^a$ = 0.200 mdyn/Å). The HBs in cluster **11** are the strongest HBs among clusters **9**–**14**. The results of the NBO analysis show that the charge of O atoms in the first hydration shell of cluster **11** is greater than the charge of O atoms of cluster **7**, due to a larger amount of charge transfer between water of the outer hydration shell and water of the inner hydration shell. As a result, the natural charges for O atoms of the inner hydration shell in cluster **11** strengthen the electrostatic interactions between the Ca ion and the inner water shell; this strengthening of the electrostatic interactions causes Ca—O interactions in cluster **11** to be shorter and stronger

than those of cluster **7** [R: 2.440 Å, BSO $n$: 0.678 (**7**); R: 2.427 Å, BSO $n$: 0.704 (**11**)].

Cluster **12** accommodates seven inner shell water molecules and three outer shell water molecules $\{[Ca(H_2O)_7]^{2+} - 3(H_2O)\}$; the interactions between the two hydration shells forge six HBs with average BSO $n$ values of 0.331 ($k^a$ = 0.186 mdyn/Å). The HBs of cluster **12** are weaker than the HBs in cluster **11** as revealed by the NBO analysis, where the charge transfer between outer shell water molecules and inner shell water molecules is slightly larger for cluster **11** than **12** [$\Delta E^{(2)}$ = 4.170 (**11**); 3.979 kcal/mol (**12**)]. The Ca—O interactions of cluster **12** are comparable in length and strength to those of cluster **11**; for cluster **12**, bond distances and electron density values of inner Ca—O interactions are slightly shorter and larger than those of **11**. In comparison to cluster **11**, the average stabilization energy ($\Delta E$) resulting from the charge transfers between the lone pairs of O atoms that comprise the first shell and lv of Ca is slightly larger for cluster **12** [$\Delta E$ = 15.029 (**11**), 15.043 kcal/mol (**12**)].

The Ca ion of cluster **13** has eight water molecules comprising the first hydration shell and a water molecule in the second hydration shell $\{[Ca(H_2O)_8]^{2+} - (H_2O)\}$; two HBs form between the first and second water shells with an average BSO $n$ of 0.331 ($k^a$ = 0.185 mdyn/Å). In comparison to cluster **8**, the average strength and length of (inner) Ca—O bonds for cluster **13** decrease (see Table I). Cluster **14** has eight and two water molecules in the first and second hydration shells $\{[Ca(H_2O)_8]^{2+} - 2(H_2O)\}$; the two water molecules of the second shell form four HBs with water of the inner shell with an average BSO $n$ value of 0.327 ($k^a$ = 0.177 mdyn/Å). The HBs of **13** are slightly stronger than those of **14** due to a greater amount of stabilization energy that results from the charge transfer between the O atoms of the second hydration shell and the O atoms of the first hydration shell [$\Delta E^{(2)}$ = 3.990 (**13**), 3.875 kcal/mol (**14**)]. The slightly stronger Ca—O interactions in **14** result from a slightly larger average stabilization energy for the electron charge transfer between the O atoms of the first hydration shell and the Ca ion [$\Delta E^{(2)}$ = 14.61 (**13**), 14.76 kcal/mol (**14**)].

### C. Cumulative local mode force constants as a predictive tool for determining the CN of hydrated calcium clusters

To determine the CN of the first hydration shell, clusters **1**–**8** were recalculated using the implicit CPCM solvation model; in this way, the first hydration shell around the $Ca^{2+}$ ion is modeled explicitly, while a second hydration shell and beyond are represented by the dielectric continuum. For these clusters, we employed the local mode analysis to determine the primary factor behind their stabilization. As shown in Table III, in terms of cumulative Ca—O and HB force constants for each cluster, the local mode analysis reveals that the six-coordinated cluster (**6**) has the strongest stabilization from the Ca—O and HB interactions compared to the other clusters. Experimental[12,21–24] and computational[28–30,36] studies essentially agree on a CN of 6 for the hydrated calcium ion cluster, as suggested from the local mode analysis results. Due to electronic reorganization and geometry relaxation, the corresponding BE values tabulated for these clusters suggest that the eight-coordinated structure is the most preferable (see Table III).

**TABLE III**. The sum of the local mode force constants $k^a$ and binding energies (BEs) for clusters **1–8** at the ωB97X-D/6-311++G(d,p) level of theory using the implicit CPCM solvation model.[a]

| Cluster | $k^a$ (mdyn/Å) | BE (kcal/mol) |
|---|---|---|
| 1 | 0.657 | −5.341 |
| 2 | 1.140 | −10.516 |
| 3 | 1.779 | −15.002 |
| 4 | 2.317 | −21.012 |
| 5 | 3.052 | −26.570 |
| 6 | 4.404 | −32.362 |
| 7 | 3.015 | −38.843 |
| 8 | 3.072 | −41.943 |

[a]The sum of the local mode force constant $k^a$ values for clusters **1–8** incorporates all corresponding $k^a$(Ca—O) values.

As shown from Table IV, the cumulative force constants, among explicitly solvated clusters **9**–**14**, are largest for cluster **9** and second largest for cluster **10** (see Table IV and Fig. 4). The cumulative force constants for explicitly solvated clusters indicate a coordination number of 5. However, the presence of additional hydration shells with explicit and implicit solvation models show that an additional hydration shell further stabilizes the hydrated calcium clusters primarily when the CN is 6; this result agrees with experimental results.

Moreover, because the largest cumulative $k^a$ values result for $[Ca(H_2O)_n]^{2+} - m(H_2O)$ clusters, where n + m = 9 (**9**, **11**, and **13**), such clusters are more likely to exist than $[Ca(H_2O)_n]^{2+} - m(H_2O)$ clusters, where n + m = 10 (**10**, **12**, and **14**). Because the BE values tabulated for explicitly solvated clusters **9–14** propose the CN to have a value of 6 in the presence of a secondary hydration shell,

**TABLE IV**. The sum of the local mode force constants $k^a$ and binding energies (BEs) for clusters **1–14** at the ωB97X-D/6-311++G(d,p) level of theory.[a]

| Cluster | $k^a$ (mdyn/Å) | BE (kcal/mol) |
|---|---|---|
| 1 | 1.147 | −55.144 |
| 2 | 2.024 | −103.215 |
| 3 | 2.685 | −145.787 |
| 4 | 3.492 | −182.743 |
| 5 | 3.705 | −212.913 |
| 6 | 3.534 | −240.471 |
| 7 | 3.023 | −258.236 |
| 8 | 2.728 | −271.730 |
| 9 | 5.202 | −300.519 |
| 10 | 4.822 | −317.053 |
| 11 | 4.077 | −297.622 |
| 12 | 4.393 | −314.890 |
| 13 | 2.950 | −291.084 |
| 14 | 3.416 | −309.897 |

[a]The sum of the local mode force constant $k^a$ values is the sum of all $k^a$(Ca—O) values for corresponding clusters **1–8**; for clusters **9–14**, the sum of the local mode force constants $k^a$ considers all $k^a$(Ca—O) and $k^a$(HB) values.

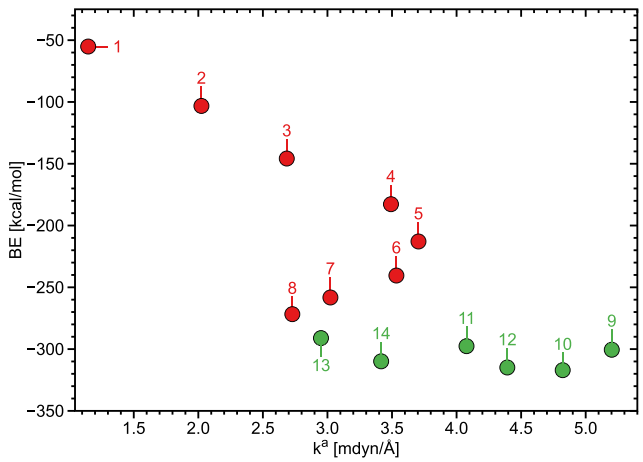


**FIG. 4**. The binding energy (BE) and the corresponding local mode force constant $k^a$ summations of clusters **1–14** calculated at the ωB97X-D/6-311++G(d,p) level of theory.

while the implicit solvation (CPCM) of clusters **1–8**, which models a secondary hydration shell, suggests a CN of 8, it is apparent that BE is not consistent as the BE values for explicit and implicit solvation of the calcium ion give different answers. Overall, the results support the notion that BE values are not adequate bond strength descriptors for hydrated calcium ion clusters as geometrical relaxation and electronic relaxation cause molecular fragments to be lower in energy than their bonded analog.

## IV. CONCLUSION

We investigated a set of 14 hydrated calcium clusters with the aim of elucidating the factors that govern the intrinsic strength of inner Ca—O (ion–solvent) and HB (solvent–solvent) interactions based on accurate ωB97X-D/6-311++G(d,p) calculations of the local stretching force constant and an analysis of NBO charges, electron density distributions, charge transfer values, and relative BSO values *n* all calculated at the ωB97X-D/6-311++G(d,p) level of theory. In this way, a clear understanding of the nature of Ca—O and HB emerged. In this study, local stretching force constants rather than BEs have been taken into account to determine the CN for the $Ca^{2+}$ ion.

1. The intrinsic strength of inner Ca—O interactions for $[Ca(H_2O)_n]^{2+}$ (n = 1–8) clusters weakens, on average, as the CN increases. The intrinsic bond strength of the inner Ca—O interactions weakens as the size of the solvation shell expands due to a decrease in electron density in the Ca—O bond region, resulting from increased charge transfer from lp(O) → lv(Ca), which weakens the electrostatic interactions between the Ca ion and O atoms of $H_2O$.
2. The strength of the HB interactions occurring between the first and second hydration shells within $[Ca(H_2O)_n]^{2+} - m(H_2O)$ (n = 6–8, m = 1–4, n + m = 9–10) clusters becomes stronger when larger amount of charge transfer occurs between HB donor atoms and HB acceptor atoms [lp(O) → $\sigma^*$(O—H)]. The HB bond interactions between the two solvent shells for hydrated calcium ion clusters were observed to be weaker than those of the water dimer by as little as 0.011 mdyn/Å and as much as 0.038 mdyn/Å.
3. The NBO charge of O atoms that comprise the first hydration shell increases due to a larger amount of charge transfer occurring between solvent shells. The increase in the charge for the O atoms of the first hydration shell strengthens the electrostatic interactions between the Ca ion and inner water molecules, enabling the Ca—O interactions to be stronger. The Ca—O bond strength for clusters involving a secondary hydration shell becomes stronger from enhanced charge transfer occurring between lp(O) → lv(Ca).
4. The cumulative local mode force constants, derived for the explicit and implicit hydration of the $Ca^{2+}$ ion, predict a CN of 6 to possess the strongest stabilization from Ca—O and HB interactions.

Comprehending the nature of Ca—O and HB intrinsic bond strengths is key to enlightening the biological roles of hydrated $Ca^{2+}$. The results of the local mode analysis confirmed that the interactions between $Ca^{2+}$ and the O atom of $H_2O$ molecules are relatively weak, allowing the hydrated calcium clusters to have fast kinetics and high flexibility, which is advantageous in controlling and maintaining many biological processes. While BE is typically used as a measure of bond strength, they are of limited use due to geometrical relaxation and electronic reorganization; thus, BE values stray away from understanding the nature of the Ca—O and HB interactions. On the other hand, the local stretching force constant, derived from the local mode analysis, is a valuable tool that adequately describes the nature of a bond. Cumulative stretching force constants can be used as a predictive tool for determining the preferred CN of hydrated calcium ion clusters.

## SUPPLEMENTARY MATERIAL

See the supplementary material for the following: The tabulated values for the calculated binding energies (BEs) for clusters **1–14**, which involve explicit water molecules, obtained at the ωB97X-D/6-311++G(d,p) level of theory, are expressed in Table S1. In Table S2, the BE values calculated in this work for clusters **9–14**, which possess explicit water molecules, are listed alongside the BE values determined for the same clusters within the work of Bai *et al.* at the B3LYP/aVDZ and MPZ/aVDZ level of theory.[35] Equations S1 and S2 were used to calculate BE values. Calculated values for interaction energies ($E_{int}$) for clusters **1–14**, which involve explicit water molecules, obtained at the ωB97X-D/6-311++G(d,p) level of theory, are expressed in Table S3. Equations S3 and S4 were used to calculate $E_{int}$ values. Table S4 shows the sum of the stabilization energy values for the charge transfer between the lone pair (lp) of the O atom of the $H_2O$ molecule and the lower valence (lv) of the Ca ion for clusters **1–8** where explicit solvation was applied. Table S5 lists the bond distances R, local mode frequencies, local mode force constants, bond strength orders, electron densities, energy densities, and energy density ratios of all OH bonds within molecules

**1**–**14**, calculated at the ωB97X-D/6-311++G(d,p) level of theory using explicit solvation. Table S6 lists the bond distances R, local mode frequencies, local mode force constants, bond strength orders, electron densities, energy densities, and energy density ratios of all CaO bonds that result from the interaction between the Ca ion and $H_2O$ molecules of the second solvent shell for clusters **9**–**14**, calculated at the ωB97X-D/6-311++G(d,p) level of theory using explicit solvation. Table S7 lists the dipole moments, bond distances R, local mode frequencies, local mode force constants, bond strength orders, electron densities, energy densities, and energy density ratios of clusters **1**–**14**, calculated at the ωB97X-D/6-311++G(d,p) level of theory using implicit solvation via the application of the CPCM solvent model. Table S8 lists the dipole moments, bond distances R, local mode frequencies, local mode force constants, bond strength orders, electron densities, energy densities, and energy density ratios for molecules **9**–**14**, calculated at the ωB97X-D/6-311++G(d,p) level of theory using implicit solvation via the application of the CPCM solvent model. Table S9 and Table S10 list the energy differences $\Delta E_{corr}$ (kcal/mol) (evaluated with zero-point correction), the change in enthalpy $\Delta H$ (kcal/mol), and the change in $\Delta G$ (kcal/mol) for all clusters **1**–**14** where Table S9 represents clusters with explicit water molecules and Table S10 depicts clusters with implicit solvation via the CPCM model; the energy difference, change in enthalpy, and change in Gibbs free energy were taken with respect to cluster **10** in both tables. Table S11 lists the atomic Cartesian coordinates in Å for clusters **1**–**14** having explicit water molecules; the coordinate values were calculated at the ωB97X-D/6-311++G(d,p) level of theory. The relationship between the averaged CaO local mode force constant values $k^a$ and corresponding BE values for clusters **1**–**14** is plotted in Fig. S1. The relationship between the CaO local mode force constant values $k^a$ and corresponding R(Ca—O) values for clusters **1**–**14** is plotted in Fig. S2. Figure S3 plots BSO $n$ (Ca—O) vs $k^a$(CaO) for **1**–**14** and **R1**-**R2**. The relationship between $k^a$(CaO) and $H_c/\rho_c$(CaO) for **1**–**14** is shown in Fig. S4. Figure S5 depicts the relationship between $k^a$(CaO) and $k^a$(HB) values for clusters **9**–**14**. In Fig. S6, the cumulative $k^a$(CaO) values are plotted against corresponding $E_{int}$ values for clusters **1**–**14**. The BE values are plotted against corresponding $E_{int}$ in Fig. S7 for clusters **1**–**14**. In Fig. S8, the cumulative $k^a$(CaO) values are plotted against corresponding $E_{corr}$ values for clusters **1**–**14**. Figures S9 and S10 plot the $k^a$(HB) values against the HB bond lengths and HB electron densities for **1**–**14**. Figure S11 shows the relationship between BE and the corresponding local mode force constant $k^a$ summations of clusters **1**–**8** calculated at the ωB97X-D/6-311++G(d,p) level of theory using the implicit conductor-like polarizable continuum model (CPCM). The natural bond orbital charges for all atoms of clusters **1**–**14** that have explicit water molecules are depicted in Figs. S12–S15.

## ACKNOWLEDGMENTS

This work was supported by the National Science Foundation, Grant No. CHE 1464906. The authors thank SMU and HPC for providing generous computational resources. Computing resources used in this work were partially provided by the National Center for High Performance Computing of Turkey (UHeM) under Grant No. 5005422018. They also thank Seth Yannacone, Marek Freindorf, Vytor Oliveira, and Roland Lindh for their advice.

## DATA AVAILABILITY

The data that support the findings of this study are available within the supplementary material.

## REFERENCES

[1]J. J. R. Fraústo da Silva and R. J. Williams, *The Biological Chemistry of the Elements: The Inorganic Chemistry of Life* (Oxford University Press, Oxford, 2004).
[2]N. Greenwood and A. Earnshaw, *Chemistry of the Elements* (Pergamon Press, Oxford, 1985).
[3]G. Mancardi, U. Terranova, and N. H. de Leeuw, "Calcium phosphate prenucleation complexes in water by means of ab initio molecular dynamics simulations," Cryst. Growth Des. **16**, 3353–3358 (2016).
[4]W. J. E. M. Habraken, J. Tao, L. J. Brylka, H. Friedrich, L. Bertinetti, A. S. Schenk, A. Verch, V. Dmitrovic, P. H. H. Bomans, P. M. Frederik, J. Laven, P. van der Schoot, B. Aichmayer, G. de With, J. J. DeYoreo, and N. A. J. M. Sommerdijk, "Ion-association complexes unite classical and non-classical theories for the biomimetic nucleation of calcium phosphate," Nat. Commun. **4**, 1507 (2013).
[5]Y. Marcus, "Effect of ions on the structure of water: Structure making and breaking," Chem. Rev. **109**, 1346–1370 (2009).
[6]J. D. Gonzalez, E. Florez, J. Romero, A. Reyes, and A. Restrepo, "Microsolvation of $Mg^{2+}$, $Ca^{2+}$: Strong influence of formal charges in hydrogen bond networks," J. Mol. Model. **19**, 1763–1777 (2013).
[7]M. Śmiechowski and I. Persson, "Hydration of oxometallate ions in aqueous solution," Inorg. Chem. **59**, 8231–8239 (2020).
[8]H. Ohtaki and T. Radnai, "Structure and dynamics of hydrated ions," Chem. Rev. **93**, 1157–1204 (1993).
[9]S. Sheweita and K. Khoshhal, "Calcium metabolism and oxidative stress in bone fractures: Role of antioxidants," Curr. Drug Metab. **8**, 519–525 (2007).
[10]V. Hengst, C. Oussoren, T. Kissel, and G. Storm, "Bone targeting potential of bisphosphonate-targeted liposomes. Preparation, characterization and hydroxyapatite binding in vitro," Int. J. Pharm. **331**, 224–227 (2007).
[11]M. B. Koirala, T. D. T. Nguyen, A. Pitchaimani, S.-O. Choi, and S. Aryal, "Synthesis and characterization of biomimetic hydroxyapatite nanoconstruct using chemical gradient across lipid bilayer," ACS Appl. Mater. Interfaces **7**, 27382–27390 (2015).
[12]D. R. Carl, R. M. Moision, and P. B. Armentrout, "Binding energies for the inner hydration shells of $Ca^{2+}$: An experimental and theoretical investigation of $Ca^{2+}(H_2O)_x$ complexes ($x$ = 5-9)," Int. J. Mass Spectrom. **265**, 308–325 (2007).
[13]M. W. Berchtold, H. Brinkmeier, and M. Müntener, "Calcium ion in skeletal muscle: Its crucial role for muscle function, plasticity, and disease," Physiol. Rev. **80**, 1215–1265 (2000).
[14]S. M. Bristow, G. D. Gamble, A. Stewart, A. M. Horne, and I. R. Reid, "Acute effects of calcium supplements on blood pressure and blood coagulation: Secondary analysis of a randomised controlled trial in post-menopausal women," Br. J. Nutr. **114**, 1868–1874 (2015).
[15]H. Bading, "Nuclear calcium signalling in the regulation of brain function," Nat. Rev. Neurosci. **14**, 593–608 (2013).
[16]H. A. Godwin, "The biological chemistry of lead," Curr. Opin. Chem. Biol. **5**, 223–227 (2001).
[17]M. Gleichmann and M. P. Mattson, "Neuronal calcium homeostasis and dysregulation," Antioxid. Redox Signaling **14**, 1261–1273 (2011).
[18]A. B. Parekh, "Calcium signaling and acute pancreatitis: Specific response to a promiscuous messenger," Proc. Natl. Acad. Sci. U. S. A. **97**, 12933–12934 (2000).
[19]P. Waring, "Redox active calcium ion channels and cell death," Arch. Biochem. Biophys. **434**, 33–42 (2005).

[20]D. Laurencin, A. Wong, J. V. Hanna, R. Dupree, and M. E. Smith, "A high-resolution $^{4}3$Ca solid-state NMR study of the calcium sites of hydroxyapatite," J. Am. Chem. Soc. **130**, 2412–2413 (2008).
[21]M. F. Bush, R. J. Saykally, and E. R. Williams, "Hydration of the calcium dication: Direct evidence for second shell formation from infrared spectroscopy," Chem. Phys. Chem. **8**, 2245–2253 (2007).
[22]M. F. Bush, R. J. Saykally, and E. R. Williams, "Infrared action spectra of $Ca^{2+}(H_2O)_{11-69}$ exhibit spectral signatures for condensed-phase structures with increasing cluster size," J. Am. Chem. Soc. **130**, 15482–15489 (2008).
[23]M. Peschke, A. T. Blades, and P. Kebarle, "Binding energies for doubly-charged ions $M^{2+}$= $Mg^{2+}$, $Ca^{2}$ + and $Zn^{2+}$ with the ligands L = $H_2O$, acetone and *N*-methylacetamide in complexes $ML_n^{2+}$ for n = 1 to 7 from gas phase equilibria determinations and theoretical calculations," J. Am. Chem. Soc. **122**, 10440–10449 (2000).
[24]R. L. Wong, K. Paech, and E. R. Williams, "Blackbody infrared radiative dissociation at low temperature: Hydration of $X^{2+}(H_2O)_n$, for X = Mg, Ca," Int. J. Mass Spectrom. **232**, 59–66 (2004).
[25]F. Jalilehvand, D. Spångberg, P. Lindqvist-Reis, K. Hermansson, I. Persson, and M. Sandström, "Hydration of the calcium ion. An EXAFS, large-angle x-ray scattering, and molecular dynamics simulation study," J. Am. Chem. Soc. **123**, 431–441 (2001).
[26]J. L. Fulton, S. M. Heald, Y. S. Badyal, and J. M. Simonson, "Understanding the effects of concentration on the solvation structure of $Ca^{2+}$ in aqueous solution. I: The perspective on local structure from EXAFS and XANES," J. Phys. Chem. A **107**, 4688–4696 (2003).
[27]E. Bruzzi and A. J. Stace, "Experimental measurements of water molecule binding energies for the second and third solvation shells of $[Ca(H_2O)_n]^{2+}$ complexes," R. Soc. Open Sci. **4**, 160671-1–160671-8 (2017).
[28]I. Bakó, J. Hutter, and G. Pálinkás, "Car-parrinello molecular dynamics simulation of the hydrated calcium ion," J. Chem. Phys. **117**, 9838–9843 (2002).
[29]X. L. Lei and B. C. Pan, "Structures, stability, vibration entropy and IR spectra of hydrated calcium ion clusters $[Ca(H_2O)_n]^{2+}$ (n = 1-20, 27): A systematic investigation by density functional theory," J. Phys. Chem. A **114**, 7595–7603 (2010).
[30]T. Megyes, T. Grósz, T. Radnai, I. Bakó, and G. Pálinkás, "Solvation of calcium ion in polar solvents: An x-ray diffraction and ab initio study," J. Phys. Chem. A **108**, 7261–7271 (2004).
[31]C. F. Schwenk, H. H. Loeffler, and B. M. Rode, "Molecular dynamics simulations of $Ca^{2+}$ in water: Comparison of a classical simulation including three-body corrections and Born-Oppenheimer *ab initio* and density functional theory quantum mechanical/molecular mechanics simulations," J. Chem. Phys. **115**, 10808–10813 (2001).
[32]D. Jiao, C. King, A. Grossfield, T. A. Darden, and P. Ren, "Simulation of $Ca^{2+}$ and $Mg^{2+}$ solvation using polarizable atomic multipole potential," J. Phys. Chem. B **110**, 18553–18559 (2006).
[33]T. Tofteberg, A. Öhrn, and G. Karlström, "Combined quantum chemical statistical mechanical simulations of $Mg^{2+}$, $Ca^{2+}$ and $Sr^{2+}$ in water," Chem. Phys. Lett. **429**, 436–439 (2006).
[34]M. M. Naor, K. V. Nostrand, and C. Dellago, "Car-parrinello molecular dynamics simulation of the calcium ion in liquid water," Chem. Phys. Lett. **369**, 159–164 (2002).
[35]G. Bai, H.-B. Yi, H.-J. Li, and J.-J. Xu, "Hydration characteristics of $Ca^{2+}$ and $Mg^{2+}$: A density functional theory, polarized continuum model and molecular dynamics investigation," Mol. Phys. **111**, 553–568 (2013).
[36]C. I. León-Pimentel, J. I. Amaro-Estrada, J. Hernández-Cobos, H. Saint-Martin, and A. Ramírez-Solís, "Aqueous solvation of Mg(II) and Ca(II): A Born-Oppenheimer molecular dynamics study of microhydrated gas phase clusters," J. Chem. Phys. **148**, 144307-1–144307-12 (2018).
[37]G. N. Merrill, S. P. Webb, and D. B. Bivin, "Formation of alkali metal/alkaline earth cation water clusters, $M(H_2O)_{1-6}$, M = $Li^+$, $Na^+$, $K^+$, $Mg^{2+}$, and $Ca^{2+}$: An effective fragment potential (EFP) case study," J. Phys. Chem. A **107**, 386–396 (2003).
[38]D. Cremer and E. Kraka, "From molecular vibrations to bonding, chemical reactions, and reaction mechanism," Curr. Org. Chem. **14**, 1524–1560 (2010).
[39]D. Setiawan, D. Sethio, D. Cremer, and E. Kraka, "From strong to weak NF bonds: On the design of a new class of fluorinating agents," Phys. Chem. Chem. Phys. **20**, 23913–23927 (2018).
[40]Y. Tao, C. Tian, N. Verma, W. Zou, C. Wang, D. Cremer, and E. Kraka, "Recovering intrinsic fragmental vibrations using the generalized subsystem vibrational analysis," J. Chem. Theory Comput. **14**, 2558–2569 (2018).
[41]A. Krapp, F. M. Bickelhaupt, and G. Frenking, "Orbital overlap and chemical bonding," Chem. Eur. J. **12**, 9196–9216 (2006).
[42]L. Zhao, M. Hermann, W. H. E. Schwarz, and G. Frenking, "The lewis electron-pair bonding model: Modern energy decomposition analysis," Nat. Rev. Chem. **3**, 48–63 (2019).
[43]D. M. Andrada, J. L. Casals-Sainz, Á. Martín Pendás, and G. Frenking, "Dative and electron-sharing bonding in $C_2F_4$," Chem. Eur. J. **24**, 9083–9089 (2018).
[44]Z. Konkoli and D. Cremer, "A new way of analyzing vibrational spectra. I. Derivation of adiabatic internal modes," Int. J. Quantum Chem. **67**, 1–9 (1998).
[45]Z. Konkoli, J. A. Larsson, and D. Cremer, "A new way of analyzing vibrational spectra. II. Comparison of internal mode frequencies," Int. J. Quantum Chem. **67**, 11–27 (1998).
[46]Z. Konkoli and D. Cremer, "A new way of analyzing vibrational spectra. III. Characterization of normal vibrational modes in terms of internal vibrational modes," Int. J. Quantum Chem. **67**, 29–40 (1998).
[47]Z. Konkoli, J. A. Larsson, and D. Cremer, "A new way of analyzing vibrational spectra. IV. Application and testing of adiabatic modes within the concept of the characterization of normal modes," Int. J. Quantum Chem. **67**, 41–55 (1998).
[48]R. Kalescky, W. Zou, E. Kraka, and D. Cremer, "Quantitative assessment of the multiplicity of carbon-halogen bonds: Carbenium and halonium ions with F, Cl, Br, and I," J. Phys. Chem. A **118**, 1948–1963 (2014).
[49]E. Kraka and D. Cremer, "Characterization of CF bonds with multiple-bond character: Bond lengths, stretching force constants, and bond dissociation energies," ChemPhysChem **10**, 686–698 (2009).
[50]R. Kalescky, E. Kraka, and D. Cremer, "Identification of the strongest bonds in Chemistry," J. Phys. Chem. A **117**, 8981–8995 (2013).
[51]A. Humason, W. Zou, and D. Cremer, "11,11-Dimethyl-1,6-methano[10] annulene-An annulene with an ultralong CC bond or a fluxional molecule?," J. Phys. Chem. A **119**, 1666–1682 (2014).
[52]V. Oliveira, D. Cremer, and E. Kraka, "The many facets of chalcogen bonding: Described by vibrational spectroscopy," J. Phys. Chem. A **121**, 6845–6862 (2017).
[53]D. Setiawan, E. Kraka, and D. Cremer, "Description of pnicogen bonding with the help of vibrational spectroscopy-the missing link between theory and experiment," Chem. Phys. Lett. **614**, 136–142 (2014).
[54]V. Oliveira, E. Kraka, and D. Cremer, "The intrinsic strength of the halogen bond: Electrostatic and covalent contributions described by coupled cluster theory," Phys. Chem. Chem. Phys. **18**, 33031–33046 (2016).
[55]V. Oliveira, E. Kraka, and D. Cremer, "Quantitative assessment of halogen bonding utilizing vibrational spectroscopy," Inorg. Chem. **56**, 488–502 (2016).
[56]V. Oliveira and D. Cremer, "Transition from metal-ligand bonding to halogen bonding involving a metal as halogen acceptor: A study of Cu, Ag, Au, Pt, and Hg complexes," Chem. Phys. Lett. **681**, 56–63 (2017).
[57]D. Sethio, V. Oliveira, and E. Kraka, "Quantitative assessment of tetrel bonding utilizing vibrational spectroscopy," Molecules **23**, 2763 (2018).
[58]S. Yannacone, D. Sethio, and E. Kraka, "Quantitative assessment of intramolecular hydrogen bonds in neutral histidine," Theor. Chem. Acc. **139**, 125–1–125–10 (2020).
[59]J. B. L. Martins, R. P. Quintino, J. R. d. S. Politi, D. Sethio, R. Gargano, and E. Kraka, "Computational analysis of vibrational frequencies and rovibrational spectroscopic constants of hydrogen sulfide dimer using MP2 and CCSD(T)," Spectrochim. Acta A **239**, 118540-1–118540-9 (2020).
[60]M. Freindorf, E. Kraka, and D. Cremer, "A comprehensive analysis of hydrogen bond interactions based on local vibrational modes," Int. J. Quantum Chem. **112**, 3174–3187 (2012).
[61]R. Kalescky, W. Zou, E. Kraka, and D. Cremer, "Local vibrational modes of the water dimer—Comparison of theory and experiment," Chem. Phys. Lett. **554**, 243–247 (2012).

[62]R. Kalescky, E. Kraka, and D. Cremer, "Local vibrational modes of the formic acid dimer—The strength of the double H-bond," Mol. Phys. **111**, 1497–1510 (2013).
[63]Y. Tao, W. Zou, J. Jia, W. Li, and D. Cremer, "Different ways of hydrogen bonding in water—Why does warm water freeze faster than cold water?," J. Chem. Theory Comput. **13**, 55–76 (2017).
[64]K. S. Thanthiriwatte, E. G. Hohenstein, L. A. Burns, and C. D. Sherrill, "Assessment of the performance of DFT and DFT-D methods for describing distance dependence of hydrogen-bonded interactions," J. Chem. Theory Comput. **7**, 88–96 (2010).
[65]J.-D. Chai and M. Head-Gordon, "Long-Range corrected hybrid density functionals with damped atom–atom dispersion corrections," Phys. Chem. Chem. Phys. **10**, 6615–6620 (2008).
[66]J.-D. Chai and M. Head-Gordon, "Systematic optimization of long-range corrected hybrid density functionals," J. Chem. Phys. **128**, 084106 (2008).
[67]R. Ditchfield, W. J. Hehre, and J. A. Pople, "Self-consistent molecular-orbital methods. IX. An extended Gaussian-type basis for molecular-orbital studies of organic molecules," J. Chem. Phys. **54**, 724–728 (1971).
[68]P. C. Hariharan and J. A. Pople, "The influence of polarization functions on molecular orbital hydrogenation energies," Theor. Chim. Acta **28**, 213–222 (1973).
[69]S. Bhattacharyya and S. Wategaonkar, "ZEKE photoelectron spectroscopy of *p*-fluorophenol···$H_2S$/$H_2O$ complexes and dissociation energy measurement using the birge-sponer extrapolation method," J. Phys. Chem. A **118**, 9386–9396 (2014).
[70]S. Brand, H. Elsen, J. Langer, S. Grams, and S. Harder, "Calcium-Catalyzed arene C-H bond activation by low-valent $Al^{I}$," Angew. Chem. **131**, 15642–15649 (2019).
[71]L. M. da Costa, S. R. Stoyanov, S. Gusarov, X. Tan, M. R. Gray, J. M. Stryker, R. Tykwinski, J. W. de M. Carneiro, P. R. Seidl, and A. Kovalenko, "Density functional theory investigation of the contributions of $\pi$–$\pi$ stacking and hydrogen-bonding interactions to the aggregation of model asphaltene compounds," Energy Fuels **26**, 2727–2735 (2012).
[72]M. Domagała and M. Palusiak, "The influence of substituent effect on non-covalent interactions in ternary complexes stabilized by hydrogen-bonding and halogen-bonding," Comput. Theor. Chem. **1027**, 173–178 (2014).
[73]D. Sutradhar, A. K. Chandra, and T. Zeegers-Huyskens, "Theoretical study of the interaction of fluorinated dimethyl ethers and the ClF and HF molecules. Comparison between halogen and hydrogen bonds," Int. J. Quantum Chem. **116**, 670–680 (2016).
[74]Y. Takano and K. N. Houk, "Benchmarking the conductor-like polarizable continuum model (CPCM) for aqueous solvation free energies of neutral and ionic organic molecules," J. Chem. Theory Comput. **1**, 70–77 (2004).
[75]A. J. L. Jesus, L. I. N. Tomé, M. E. S. Eusébio, M. T. S. Rosado, and J. S. Redinha, "Hydration of cyclohexylamines: CPCM calculation of hydration Gibbs energy of the conformers," J. Phys. Chem. A **111**, 3432–3437 (2007).
[76]E. B. Wilson, J. C. Decius, and P. C. Cross, *Molecular Vibrations. The Theory of Infrared and Raman Vibrational Spectra* (McGraw-Hill, New York, 1955).
[77]W. Zou, R. Kalescky, E. Kraka, and D. Cremer, "Relating normal vibrational modes to local vibrational modes with the help of an adiabatic connection scheme," J. Chem. Phys. **137**, 084114 (2012).
[78]E. Kraka, J. A. Larsson, and D. Cremer, "Generalization of the badger rule based on the use of adiabatic vibrational modes," in *Computational Spectroscopy*, edited by J. Grunenberg (Wiley, New York, 2010), pp. 105–149.
[79]M. J. Frisch, G. W. Trucks, H. B. Schlegel, G. E. Scuseria, M. A. Robb, J. R. Cheeseman, G. Scalmani, V. Barone, G. A. Petersson, H. Nakatsuji, X. Li, M. Caricato, A. V. Marenich, J. Bloino, B. G. Janesko, R. Gomperts, B. Mennucci, H. P. Hratchian, J. V. Ortiz, A. F. Izmaylov, J. L. Sonnenberg, D. Williams-Young, F. Ding, F. Lipparini, F. Egidi, J. Goings, B. Peng, A. Petrone, T. Henderson, D. Ranasinghe, V. G. Zakrzewski, J. Gao, N. Rega, G. Zheng, W. Liang, M. Hada, M. Ehara, K. Toyota, R. Fukuda, J. Hasegawa, M. Ishida, T. Nakajima, Y. Honda, O. Kitao, H. Nakai, T. Vreven, K. Throssell, J. A. Montgomery, Jr., J. E. Peralta, F. Ogliaro, M. J. Bearpark, J. J. Heyd, E. N. Brothers, K. N. Kudin, V. N. Staroverov, T. A. Keith, R. Kobayashi, J. Normand, K. Raghavachari, A. P. Rendell, J. C. Burant, S. S. Iyengar, J. Tomasi, M. Cossi, J. M. Millam, M. Klene, C. Adamo, R. Cammi, J. W. Ochterski, R. L. Martin, K. Morokuma, O. Farkas, J. B. Foresman, and D. J. Fox, Gaussian~16 Revision C.01, Gaussian, Inc., Wallingford, CT, 2016.
[80]E. Kraka, W. Zou, M. Filatov, Y. T. J. Gräfenstein, D. Izotov, J. Gauss, Y. He, A. Wu, Z. Konkoli *et al.*, COLOGNE2019, 2019, available at: http://www.smu.edu/catco; accessed on 23 December 2019.
[81]F. Weinhold and C. R. Landis, *Valency and Bonding: A Natural Bond Orbital Donor-Acceptor Perspective* (Cambridge University Press, Cambridge, 2005).
[82]A. E. Reed, L. A. Curtiss, and F. Weinhold, "Intermolecular interactions from a natural bond orbital, donor-acceptor viewpoint," Chem. Rev. **88**, 899–926 (1988).
[83]T. A. Keith, TK Gristmill Software, aim.tkgristmill.com, Overland Park KS, USA, 2019.
[84]D. Cremer and E. Kraka, "Chemical bonds without bonding electron density? Does the difference electron-density analysis suffice for a description of the chemical bond?," Angew. Chem., Int. Ed. **23**, 627–628 (1984).
[85]D. Cremer and E. Kraka, "A description of the chemical bond in terms of local properties of electron density and energy," Croa. Chem. Acta **57**, 1259–1281 (1984), https://hrcak.srce.hr/194019.
[86]E. Kraka and D. Cremer, "Chemical implication of local features of the electron density distribution," in *Theoretical Models of Chemical Bonding*, The Concept of the Chemical Bond Vol. 2, edited by Z. B. Maksic (Springer-Verlag, Heidelberg, 1990), p. 453.
[87]G. Ren, Y. Ha, Y.-S. Liu, X. Feng, N. Zhang, P. Yu, L. Zhang, W. Yang, J. Feng, J. Guo, and X. Liu, "Deciphering the solvent effect for the solvation structure of $Ca^{2+}$ in polar molecular liquids," J. Phys. Chem. B **124**, 3408–3417 (2020).
[88]Y. Tao, W. Zou, and E. Kraka, "Strengthening of hydrogen bonding with the push-pull effect," Chem. Phys. Lett. **685**, 251–258 (2017).